



Large Wind Turbine Rotor Design using an Aero-Elastic / Free-Wake Panel Coupling Code

Sessarego, Matias; Ramos García, Néstor; Shen, Wen Zhong; Sørensen, Jens Nørkær

Published in:
Journal of Physics: Conference Series (Online)

Link to article, DOI:
[10.1088/1742-6596/753/4/042017](https://doi.org/10.1088/1742-6596/753/4/042017)

Publication date:
2016

Document Version
Publisher's PDF, also known as Version of record

[Link back to DTU Orbit](#)

Citation (APA):
Sessarego, M., Ramos García, N., Shen, W. Z., & Sørensen, J. N. (2016). Large Wind Turbine Rotor Design using an Aero-Elastic / Free-Wake Panel Coupling Code. *Journal of Physics: Conference Series (Online)*, 753, [042017]. DOI: 10.1088/1742-6596/753/4/042017

DTU Library

Technical Information Center of Denmark

General rights

Copyright and moral rights for the publications made accessible in the public portal are retained by the authors and/or other copyright owners and it is a condition of accessing publications that users recognise and abide by the legal requirements associated with these rights.

- Users may download and print one copy of any publication from the public portal for the purpose of private study or research.
- You may not further distribute the material or use it for any profit-making activity or commercial gain
- You may freely distribute the URL identifying the publication in the public portal

If you believe that this document breaches copyright please contact us providing details, and we will remove access to the work immediately and investigate your claim.

Large Wind Turbine Rotor Design using an Aero-Elastic / Free-Wake Panel Coupling Code

This content has been downloaded from IOPscience. Please scroll down to see the full text.

2016 J. Phys.: Conf. Ser. 753 042017

(<http://iopscience.iop.org/1742-6596/753/4/042017>)

View [the table of contents for this issue](#), or go to the [journal homepage](#) for more

Download details:

IP Address: 192.38.89.35

This content was downloaded on 08/10/2016 at 16:23

Please note that [terms and conditions apply](#).

You may also be interested in:

[On the aero-elastic design of the DTU 10MW wind turbine blade for the LIFES50+ wind tunnel scale model](#)

I. Bayati, M. Belloli, L. Bernini et al.

[Sensitivity of Key Parameters in Aerodynamic Wind Turbine Rotor Design on Power and Energy Performance](#)

Christian Bak

[Aerodynamic and Structural Design of MultiMW Wind Turbine Blades beyond 5MW](#)

B Hillmer, T Borstelmann, P A Schaffarczyk et al.

[OC3—Benchmark Exercise of Aero-elastic Offshore Wind Turbine Codes](#)

P Passon, M Kühn, S Butterfield et al.

[Aerofoil flutter: fluid-mechanical analysis and wind tunnel testing](#)

A L Wensuslaus and A J McMillan

[Operating wind turbines in strong wind conditions by using feedforward-feedback control](#)

Ju Feng and Wen Zhong Sheng

Large Wind Turbine Rotor Design using an Aero-Elastic / Free-Wake Panel Coupling Code

Matias Sessarego, Néstor Ramos-García, Wen Zhong Shen, Jens Nørkær Sørensen

Department of Wind Energy, Fluid Mechanics Section, Building 403, Technical University of Denmark, DK-2800 Lyngby, Denmark

E-mail: matse@dtu.dk

Abstract. Despite the advances in computing resources in the recent years, the majority of large wind-turbine rotor design problems still rely on aero-elastic codes that use blade element momentum (BEM) approaches to model the rotor aerodynamics. The present work describes an approach to wind-turbine rotor design by incorporating a higher-fidelity free-wake panel aero-elastic coupling code called MIRAS-FLEX. The optimization procedure includes a series of design load cases and a simple structural design code. Due to the heavy MIRAS-FLEX computations, a surrogate-modeling approach is applied to mitigate the overall computational cost of the optimization. Improvements in cost of energy, annual energy production, maximum flap-wise root bending moment, and blade mass were obtained for the NREL 5MW baseline wind turbine.

1. Introduction

Wind-turbine blade design is a complex iterative process, which requires knowledge in several areas of engineering. In the past, blade plan-form design was performed using simple analytical expressions based on wind-turbine rotor aerodynamics only, see e.g. [1] and [2]. Today, the advances in computing resources have permitted solution of sophisticated numerical optimization problems involving two or more disciplines in the design process [3, 4]. Despite the advances in computing techniques in the recent years, the majority of blade design problems still rely on aero-elastic codes that use blade element momentum (BEM) approaches to model the rotor aerodynamics. The present work describes an approach to wind-turbine rotor design by incorporating a higher-fidelity free-wake panel aero-elastic coupling code called MIRAS-FLEX [5].

The work objectives were:

- (i) To develop an efficient optimization framework for wind-turbine blade design using a high-fidelity aero-elastic model;
- (ii) To create a preliminary design of a 5MW wind-turbine blade using the developed design framework.

2. Methodology

This section describes the methodology used in the large wind-turbine rotor design framework. First, the optimization problem is shown, then the MIRAS-FLEX code, structural design code,



and surrogate modeling components of the framework are described.

2.1. Optimization problem

The design objective is to minimize the cost of energy (COE):

$$\begin{aligned}
 & \underset{x}{\text{minimize}} && \frac{\text{COE}}{\text{COE}_{\text{ref}}} \\
 & \text{subject to} && \mathbf{x} \in \mathbb{R}^n, \\
 & && g_c(\mathbf{x}) \leq 0, \\
 & && x_k^L \leq x_k \leq x_k^U, k = 1, \dots, n
 \end{aligned} \tag{1}$$

where the subscript, ref, denotes the reference blade. The vector \mathbf{x} contains a total of n variables that are real numbers, \mathbb{R} . The design variables, $\mathbf{x} = [x_1, x_2, \dots, x_n]$, are control points (CPs) that define the chord, twist and relative thickness as a function of blade span, see Figure 1. B-splines [6] are used to parameterize the chord and twist distributions, while linear interpolation is used for the relative thickness distribution. Only two CPs each for the chord, twist, and relative thickness distributions at the outboard of the blade are optimized. The upper (U) and lower (L) notations, $x_k^L \leq x_k \leq x_k^U$, are the upper and lower limits of the CPs, while the non-linear inequality constraint, $g_c \leq 0$, is to promote monotonically decreasing chord, twist, and relative thickness. The boundary and non-linear inequality constraints are required to ensure feasible blade designs.

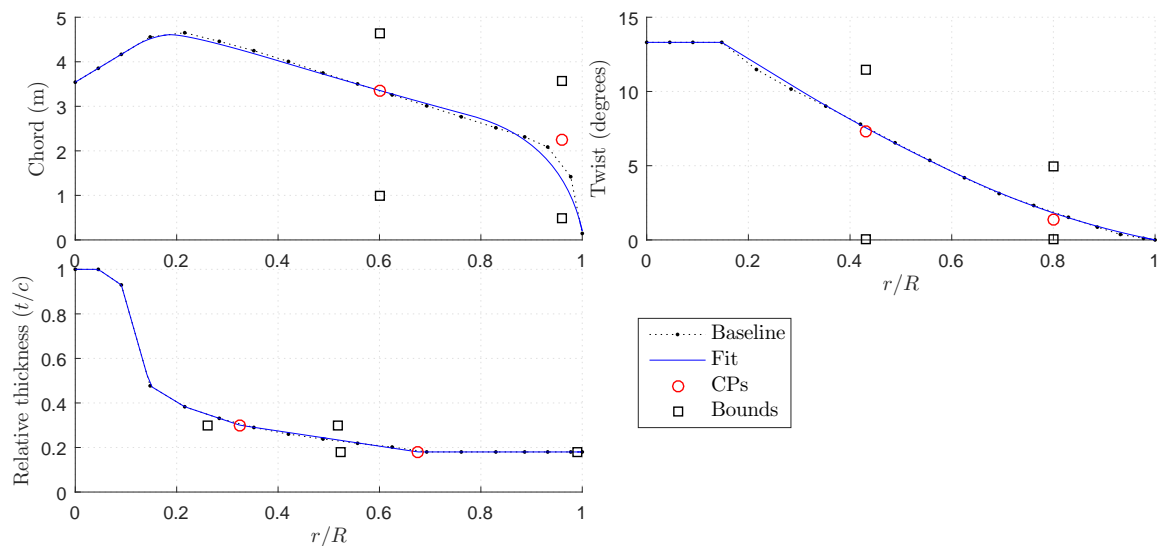


Figure 1. Blade geometry parameterization method fitted to the NREL 5MW baseline wind turbine [7], where r/R is the normalized blade radius.

Following [8], COE is calculated as:

$$\text{COE} = \frac{\text{FCR} \cdot (\text{TCC} + \text{BOS})}{\text{AEP}} + \text{AOE} \tag{2}$$

where FCR is fixed charge rate, TCC is turbine capital cost, BOS is balance of station, AOE is annual operating expenses, and AEP is annual energy production. FCR, TCC, and BOS are obtained from the NREL Wind Turbine Design Cost and Scaling Model [8]. AOE was neglected

because it gives an incentive to reduce AEP, see underlying equations in [8]. MIRAS-FLEX is used to compute AEP, see subsection 2.2, while a code based on classical laminate theory called PreComp [9] to compute the blade mass, see subsection 2.3. The rotor mass was computed from PreComp instead of the scaling law in [8] to estimate TCC.

2.2. Higher-fidelity aero-elastic code: MIRAS-FLEX

The aero-elastic code, MIRAS-FLEX [5], is composed of a free-wake panel code called MIRAS [10], and the elastic beam model of FLEX5 [11], see Figure 2. MIRAS is used to compute the aerodynamic flow solution while FLEX5 predicts the structural dynamics. MIRAS-FLEX uses a predictor-corrector and loosely-coupled approach to couple 22 degrees of freedom (DOFs) from FLEX5 with MIRAS. MIRAS will be described first, then FLEX5.

Method for Interactive Rotor Aerodynamic Simulations, MIRAS, is a three-dimensional (3D) viscous-inviscid interactive solver for horizontal-axis wind turbine (HAWT) computations. The solver predicts the aerodynamic behavior of wind-turbine wakes and blades for steady and unsteady conditions. The MIRAS code consists of an inviscid and a viscous part. The inviscid part is a 3D panel method using a surface distribution of quadrilateral sources and doublets. The viscous part is solved in blade cross-sections using the integral viscous boundary layer solver, Q³UIC [12]. Transpiration velocity data from Q³UIC is used to modify the inviscid solution from MIRAS and take the viscous effects into account. A free-wake model simulates the wake behind the wind-turbine rotor using vortex filaments that carry the vorticity shed by the blades trailing edges. The MIRAS code is parallelized using message passing interface (MPI) software from Oracle Solaris Studio version 12.3 [13].

FLEX5 is an aero-elastic program developed by Øye [11] to model the dynamic behavior of HAWTs operating in specified wind conditions, such as simulated turbulent wind. The program runs in the time-domain producing time-series of loads and deflections. Aerodynamics are calculated using the BEM method with additional models important for unsteady and yaw and/or tilt conditions. Such models include dynamic wake and dynamic stall models, see e.g. [14–16]. The structural behavior of the wind turbine is modeled using the principle of virtual work and carefully selected DOFs. Modal shape functions are used for the deflections of the blades and tower, while stiff bodies connected by flexible hinges model the nacelle, rotor shaft, and hub. FLEX5 contains a total of 28 DOFs, where six of the 28 DOFs describe the deformations of a flexible foundation which are not used in the present work.

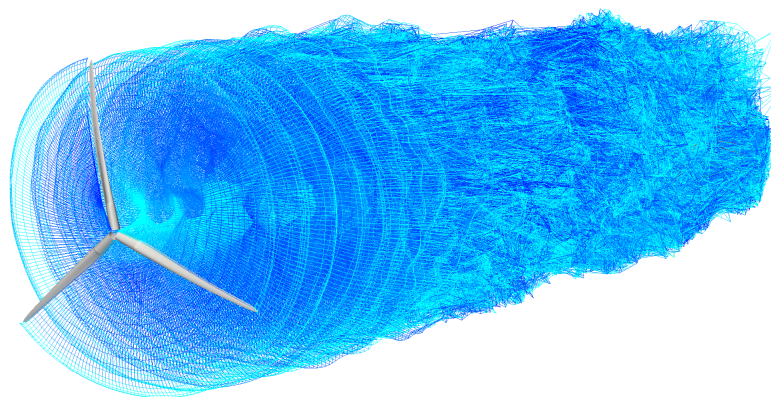


Figure 2. MIRAS-FLEX simulation with turbulent inflow.

2.3. Structural design code

A simple optimization tool to design the internal structure of large wind-turbine blades has been developed and included in the rotor design framework. The tool uses a combination of the classical laminate theory using a shear flow approach to compute blade structural properties, PreComp [9], a finite-element code to compute the blade coupled mode shapes, BModes [17], the Euler-Bernoulli beam theory to compute blade deflections and strains [18], and the BEM-based aero-elastic code FLEX5 to compute the design load cases (DLCs). The objective is to minimize the blade mass subject to a number of boundary and non-linear inequality constraints:

$$\begin{aligned}
 & \underset{\mathbf{y}}{\text{minimize}} && \text{Blade Mass} \\
 & \text{subject to} && \mathbf{y} \in \mathbb{R}^n, \\
 & && (3\omega_{\text{rotor}} SF - \omega(\mathbf{y}))/\omega_{\text{rotor}} \leq 0, \\
 & && (\delta_{\text{tip}}(\mathbf{y}) - \delta_{\text{max}})/\delta_{\text{max}} \leq 0, \\
 & && (\epsilon_{\text{tension}}(\mathbf{y}) SF - \epsilon_{\text{ultimate,tension}})/\epsilon_{\text{ultimate,tension}} \leq 0, \\
 & && (\epsilon_{\text{compression}}(\mathbf{y}) SF - \epsilon_{\text{ultimate,compression}})/\epsilon_{\text{ultimate,compression}} \leq 0, \\
 & && (\eta(\mathbf{y}) - \eta_{\text{max}})/\eta_{\text{max}} \leq 0, \\
 & && y_k^L \leq y_k \leq y_k^U, k = 1, \dots, n
 \end{aligned} \tag{3}$$

where $3\omega_{\text{rotor}}$ is the rotor blade passing frequency, SF is a safety factor, δ_{max} is the maximum allowable tip deflection, $\epsilon_{\text{ultimate,tension}}$ and $\epsilon_{\text{ultimate,compression}}$ are the ultimate tensile and compressive strain, respectively, and η_{max} is the maximum allowable buckling coefficient set to 0.5. The buckling coefficient, η , is computed for the spar-caps only, and assumes that the spar-beam is modeled as a long orthotropic plate under uni-axial compression with all edges simply supported [19]. Skin and panel buckling are not considered. The tip deflection, δ_{tip} , as well as the tensile ($\epsilon_{\text{tension}}$) and compressive ($\epsilon_{\text{compression}}$) strain are calculated from Euler-Bernoulli beam theory. The natural frequencies for the first flap-wise and edge-wise blade modes, ω , are obtained from BModes. All constraints are scaled to prevent bias and improve optimizer performance.

A box-spar layup is assumed for the internal blade structure, where the design variables, \mathbf{y} , are the spar-cap thickness and web layup (or spar width), see Figures 3 and 4. The spar-cap thickness distribution is defined by eight CPs, while the web layup is defined by the chord-wise locations of the two span-wise endpoints for each web (i.e. four CPs for a two-web layup). Linear interpolation is performed to obtain values in-between the CPs. Upper (y_k^U) and lower (y_k^L) bounds of the spar-caps and webs are used to prevent them from merging into each other and into different sectors of the cross-section, as well as becoming negative.

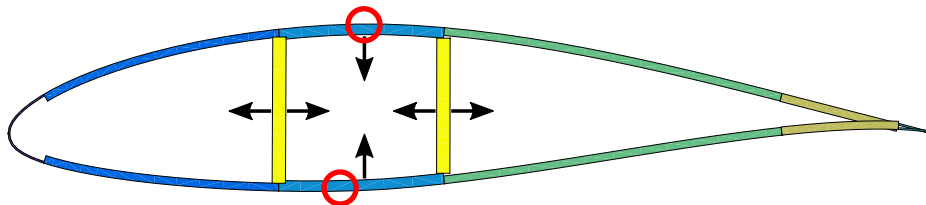


Figure 3. Drawing of the cross-section where the variables are the spar-cap thickness and the chord-wise location of the webs (arrows). Only the highest and lowest points on the airfoil contour (circles) are used to compute the strain constraint, see Problem (3).

The structural design code begins by tuning the generator and pitch controller as outlined in [21]. Then, a series of DLCs based on Resor [20] and the IEC 61400-1 standards [22] are

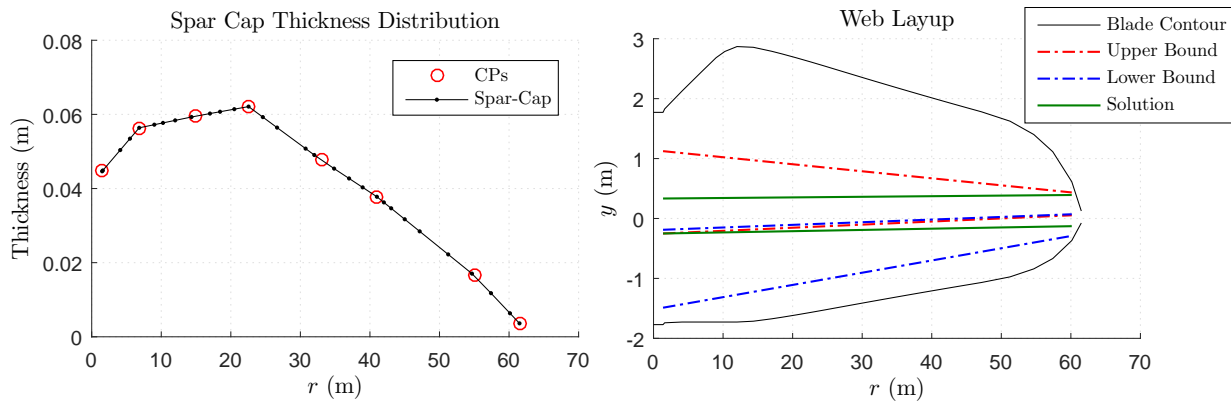


Figure 4. Optimal spar-cap thickness (left) and web layout (right) for the NREL 5MW baseline wind turbine [7, 20].

computed, see Table 1. Both the control tuning as well as the DLC computations are performed using FLEX5 and assuming stiff blades. MIRAS-FLEX is not used here because a significant portion of the cluster is needed to perform the task quickly in parallel (i.e. cluster needs to be shared with other users). Turbulent wind during normal and abnormal turbine operation was not considered. For the preliminary blade design stage, steady wind models are used in this paper for simplicity and speed. DLC 6.1 and 6.3 are computed in 5° yaw error increments/decrements ranging from 30° and -30° (i.e. 13 load cases in total for DLC 6.1 and 6.3). The bending moments normal and tangential to the rotor plane from all DLCs are collected to determine the most impactful load cases. The worst-case loads are then transferred to the optimizer, which calls a structural module for a number of iterations to find the minimum blade mass. The inputs to the structural module are the DLC loads and \mathbf{y} . The vector \mathbf{y} is used to create a structural layout and compute the objective, while the DLC loads together with the blade structural properties are used to compute the structural constraints. The MATLAB optimizer, *fmincon* [23], modifies \mathbf{y} to minimize the objective up to at least a local minimum and also satisfy all constraints.

Notice that the design of the controller as well as the inner structure are based on a rigid turbine, see Figure 5. In a fully aero-elastic design approach, Steps 2 to 4 should be repeated until convergence, where the blade stiffness distributions found from Step 4 are used to update the stiffness distributions used in Steps 2 and 3. Although not too difficult to implement, the fully aero-elastic design approach was omitted for simplicity, robustness, and faster code execution.

2.4. Surrogate modeling

MIRAS-FLEX requires much more computational time than BEM-based aero-elastic codes. Therefore, the number of calls to MIRAS-FLEX in a numerical optimization problem must be kept to a minimum. Surrogate optimization uses a mathematical model for searching local or global optima rather than the black-box function directly [24]. When a black-box function is computationally expensive, e.g. MIRAS-FLEX, surrogate optimization can achieve significant savings in computational time compared to conventional optimization methods [24]. A surrogate-based optimization code developed by the authors [25] is used in the present blade design framework. In general, surrogate-based optimization consists of three steps to find the minimum of a function:

- (i) creating a sampling plan;

Table 1. Design load cases used in the structural design code based on [20] and [22].

Design situation	DLC	Wind condition	Other conditions	Type of analysis
Normal Power Production (steady)	-	Steady Windspeed	2 m/s increments from cut-in = 3 m/s to cut-out = 25 m/s	Ultimate strength
	1.4	Extreme Coherent gust with Direction change (ECD)	Rated wind ± 2 m/s, 2 m/s spacing	Ultimate strength
	2.3 ¹	Extreme Operating Gust (EOG)	Rated wind ± 2 m/s, 2 m/s spacing	Ultimate strength
Parked (standing still or idling)	6.1	Extreme Windspeed Model (EWM) 50-year recurrence period	Yaw error $\pm 15^\circ$, 5° spacing	Ultimate strength
	6.3	EWM 1-year recurrence period	Extreme yaw misalignment, $\pm 30^\circ$	Ultimate strength

¹ Without external or internal electrical fault including loss of electrical network.

- (ii) constructing a surrogate, and;
- (iii) searching and exploiting the surrogate.

The sampling plan is created using the Latin hypercube sampling technique [25, 26], the surrogate is constructed using a radial basis function, and prediction-based exploitation [25, 26] is used to search and exploit the surrogate. A radial basis function is expressed as:

$$\hat{f}(\mathbf{x}) = \mathbf{w}^T \boldsymbol{\psi} = \sum_{i=1}^{n_c} w_i \psi(\|\mathbf{x} - \mathbf{c}^{(i)}\|) \quad (4)$$

where \hat{f} is the surrogate approximation to the scalar-valued objective function, f (see Problem (1)), \mathbf{x} is the design variable vector, \mathbf{w} is a vector containing the values of the weight coefficients w_i from $i = 1, \dots, n_c$, and $\boldsymbol{\psi}$ is the n_c -vector containing the values of the basis functions ψ . A cubic basis function, $\psi(r_b) = r_b^3$, is used where $r_b = \|\mathbf{x} - \mathbf{c}^{(i)}\|$ is from Equation 4. The values of the basis functions are evaluated at the Euclidean distances between the prediction site \mathbf{x} and the centers $\mathbf{c}^{(i)}$ of the basis functions. A unique solution for \mathbf{w} in the above equation can be determined when n_c is equal to the number of sampled points and using the *Gram matrix* [26]. Each candidate blade design in steps i) and iii) above goes through six stages to determine the COE, see Figure 5.

3. Results

Table 2 and Figure 6 (top) depict the results from the optimization of Problem (1) using the NREL 5MW baseline wind turbine [7, 20] as the reference and MIRAS-FLEX to compute the AEP. Table 3 and Figure 6 (bottom) depict the results when a simple BEM code [18] is used instead of MIRAS-FLEX. Airfoils are comprised of a cylinder, Delft University (DU) airfoils, and a NACA airfoil as described in [7]. The reference structural layup is obtained from [20]. Rotor radius and tip speed are kept the same throughout the optimization. A Weibull probability distribution with shape and scale parameters of $k = 2.48$ and $A = 7.68$ m/s, respectively, was used to calculate the AEP. The total computational time for the MIRAS-FLEX and BEM based optimizations are approximately 56 and 7 hours, respectively. Note the framework has not been

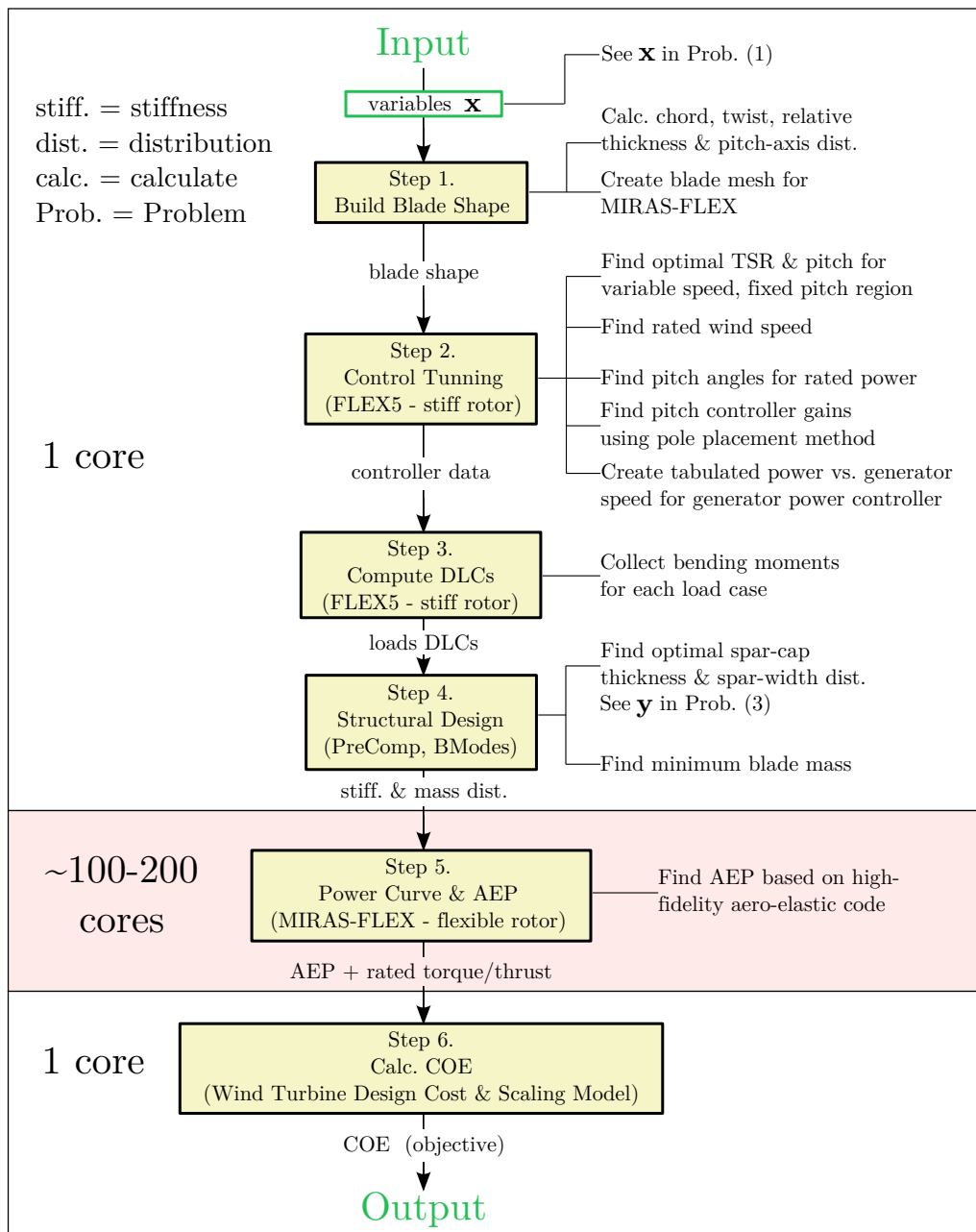


Figure 5. Flowchart for evaluating a candidate blade design comprised of six steps: 1) Build blade shape, 2) control tuning, 3) compute DLCs, 4) structural design, 5) compute AEP, and 6) calculate COE.

optimized for speed, therefore the computational times given should be interpreted as maximum values.

Table 2 and Table 3 show the results of COE, AEP, maximum flap-wise root-bending moment experienced in the DLCs (M_{flap}), thrust at rated wind speed (T_{rated}), and blade mass in tonnes (m_{blade}). Table 2 shows +1.89%, +1.87%, +5.47%, +0.19%, and +0.75% improvements for COE, AEP, M_{flap} , T_{rated} , and m_{blade} , respectively, for the MIRAS-FLEX case. When using simple BEM, Table 3 shows +0.85%, +0.72%, +2.71%, +2.35%, and +1.95%, respectively. Figure 7

Table 2. Results from the optimization of Problem (1) for the MIRAS-FLEX case.

Quantity	COE (\$/kWh)	AEP (GWh/year)	M_{flap} (MN.m)	T_{rated} (MN)	m_{blade} (tonnes)
Reference Fit	0.08401	18.5982 ²	21.235	0.64811	16.98735
Optimized	0.08242	18.94690 ²	20.074	0.64691	16.85920
% Improvement	+1.89%	+1.87%	+5.47%	+0.19%	+0.75%

² The wake was cut short to reduce computing time, therefore AEP for MIRAS-FLEX is larger than BEM. Consequently, COE for MIRAS-FLEX will be less than BEM as well, see Equation (2).

depicts the exterior shape and interior structure of the blade for the baseline, MIRAS-FLEX solution, and BEM solution. The spar-cap thickness and web layup are plotted in Figure 8 for the MIRAS-FLEX (top) and BEM (bottom) solutions, respectively. Comparing the two designs in Figure 6, differences are mainly seen at the blade tip for the chord distribution. The MIRAS-FLEX solution has a sharp blade tip, while the BEM solution does not. Detailed investigation of the local blade aerodynamics during power production and the DLCs is needed to determine the cause for the sharp blade tip. It is worth noting that very different approaches are used to model the flow near the tip in MIRAS and BEM.

Table 3. Results from the optimization of Problem (1) for the BEM case.

Quantity	COE (\$/kWh)	AEP (GWh/year)	M_{flap} (MN.m)	T_{rated} (MN)	m_{blade} (tonnes)
Reference Fit	0.08781	17.79432	21.235	0.67325	16.98735
Optimized	0.08706	17.92297	20.660	0.65744	16.65589
% Improvement	+0.85%	+0.72%	+2.71%	+2.35%	+1.95%

4. Conclusions

The majority of blade design problems rely on aero-elastic codes that use blade element momentum (BEM) approaches to model the rotor aerodynamics. The present work describes an approach to wind-turbine rotor design by incorporating a higher-fidelity free-wake panel aero-elastic code called MIRAS-FLEX. A framework comprised of MIRAS-FLEX, a structural design code, and a surrogate-based numerical optimization technique has been developed and applied to optimize the NREL 5MW baseline wind-turbine rotor. Comparisons were made by using MIRAS-FLEX and a simple BEM code to compute the annual energy production. Reductions in cost of energy were obtained for both cases.

Acknowledgments

The work was funded by the Danish Council for Strategic Research under the project name OffWindChina (Sagsnr. 0603-00506B). Computations were performed on Jess, the high performance computing cluster at Risø Campus, Technical University of Denmark.

References

- [1] Wilson R E and Lissaman P B S 1974 *Applied aerodynamics of wind power machines* (Corvallis: Oregon State University)
- [2] Burton Tony J N S D and Bossanyi E 2011 *Wind Energy Handbook* 2nd ed (Wiley)

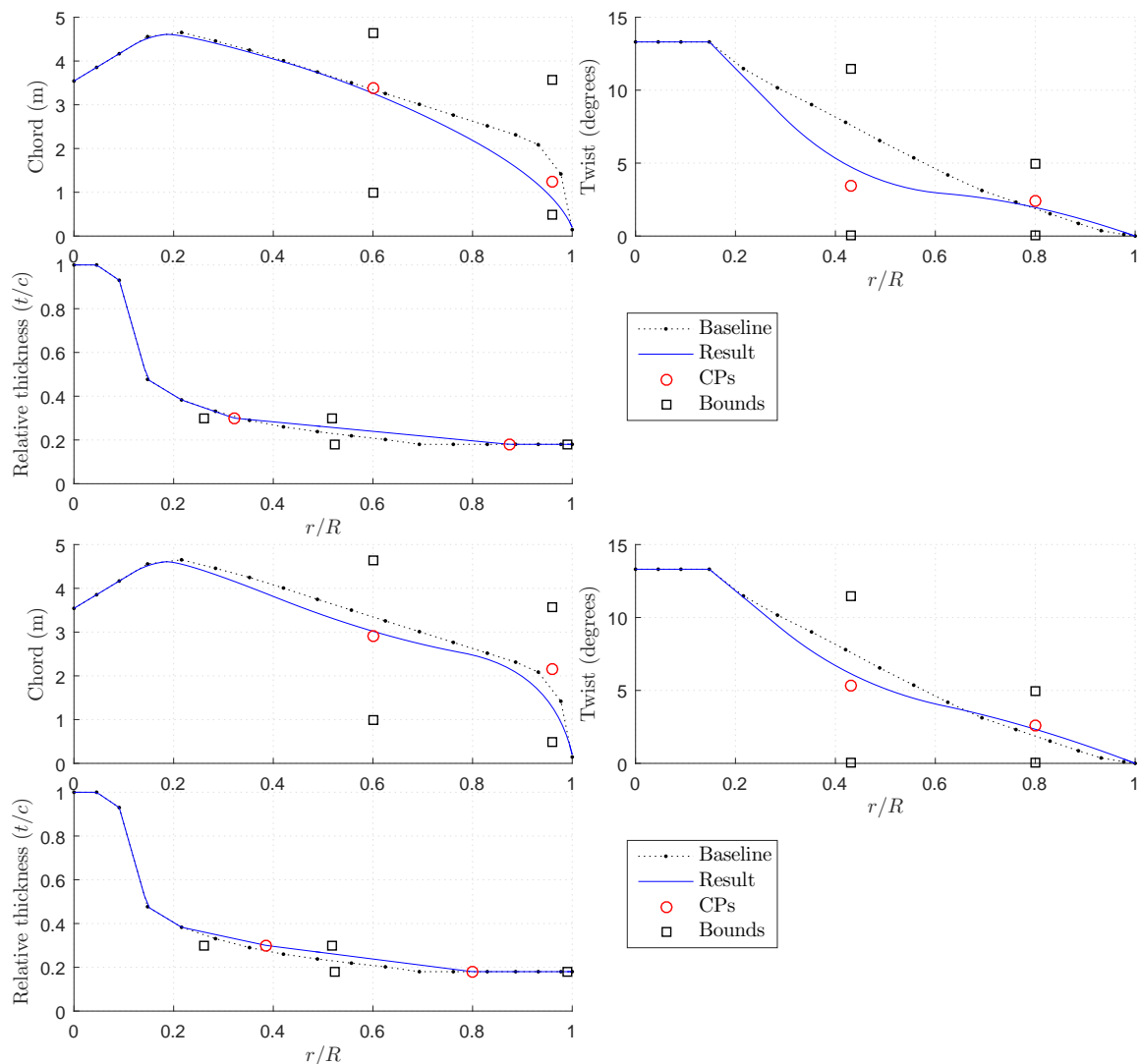


Figure 6. Blade geometry results where r/R is the normalized blade radius using MIRAS-FLEX (top) and simple BEM (bottom).

- [3] Ashuri T, Zaaijer M, Martins J, van Bussel G and van Kuik G 2014 *Renewable Energy* **68** 893–905 ISSN 09601481
- [4] Bottasso C, Campagnolo F and Croce A 2012 *Multibody System Dynamics* **27** 21–53 ISSN 1384-5640
- [5] Sessarego M, Ramos-García N and Shen W 2015 *Journal of Power and Energy Engineering* **3** 1–6 ISSN 2327-588X
- [6] Piegł L and Tiller W 1997 *The NURBS Book (2nd Ed.)* (New York, NY, USA: Springer-Verlag New York, Inc.) ISBN 3-540-61545-8
- [7] Jonkman J, Butterfield S, Musial W and Scott G 2009 Definition of a 5-MW reference wind turbine for offshore system development Tech. rep. National Renewable Energy Laboratory 1617, Cole Blvd, Golden, CO 80401
- [8] Fingerish L, Hand M and Laxson A 2006 Wind turbine design cost and scaling model Tech. rep. National Renewable Energy Laboratory 1617, Cole Blvd, Golden, CO 80401
- [9] Bir G S 2005 *User's Guide to PreComp: Pre-Processor for Computing Composite Blade Properties* National Renewable Energy Laboratory 1617, Cole Blvd, Golden, CO 80401
- [10] Ramos-García N, Sørensen J N and Shen W Z 2016 *Wind Energy* **19** 67–93 ISSN 1099-1824 URL <http://dx.doi.org/10.1002/we.1821>
- [11] Øye S 1996 *Proceedings of 28th IEA Meeting of Experts Concerning State of the Art of Aeroelastic Codes for*

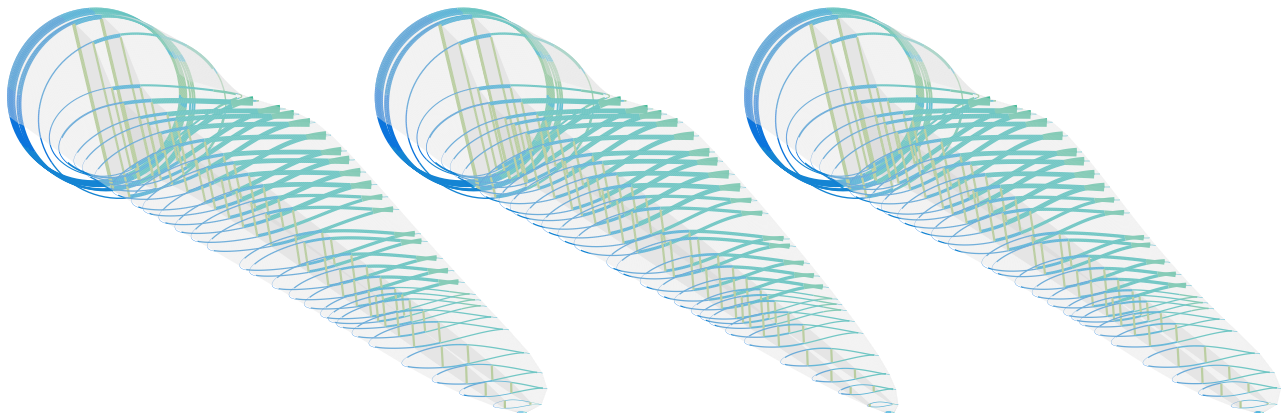


Figure 7. Blade shape and internal structure for the baseline (left), MIRAS-FLEX solution (middle) and BEM solution (right).

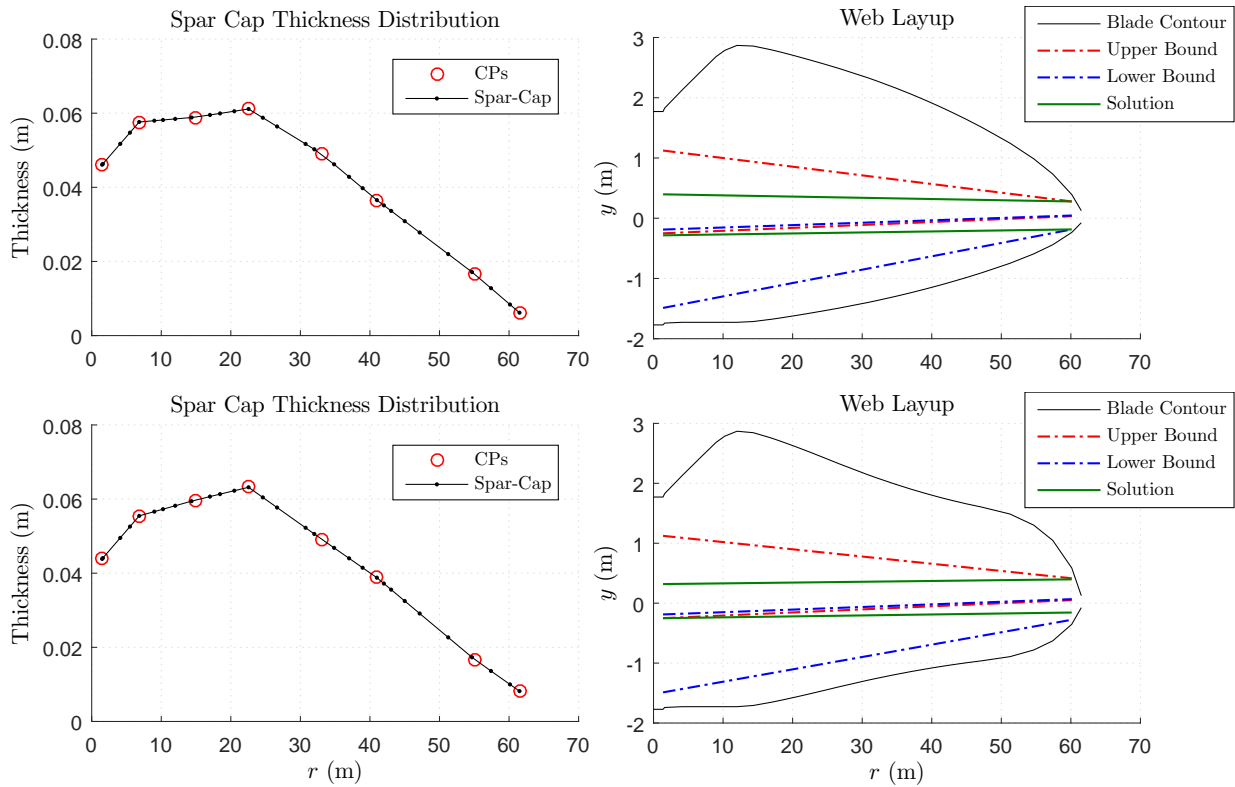


Figure 8. Spar-cap thickness (left) and web layout (right) for the MIRAS-FLEX (top) and BEM (bottom) solutions.

Wind Turbine Calculations (Lyngby: International Energy Agency)

[12] Ramos-García N, Sørensen J N and Shen W Z 2013 *Wind Energy* ISSN 1099-1824 URL <http://dx.doi.org/10.1002/we.1677>

[13] Oracle Corporation 500 Oracle Parkway, Redwood Shores, CA 94065 *Oracle Solaris Studio* URL <http://www.oracle.com>

[14] Øye S 1991 *Proceedings of the 4th IEA Symposium on the Aerodynamics of Wind Turbines* ed McAnulty K F (Harwell Laboratory, Harwell, UK: ETSU-N-118)

[15] Schepers J G and Snel H 1995 Dynamic inflow: Yawed conditions and partial span pitch control Tech. rep.

- ECN-C- -95-056 Petten, The Netherlands
- [16] Snel H and Schepers J G 1995 Joint investigation of dynamic inflow effects and implementation of an engineering method Tech. rep. ECN-C- -94-107 Petten, The Netherlands
- [17] Bir G S 2007 *User's Guide to BModes (Software for Computing Rotating Beam Coupled Modes)* National Renewable Energy Laboratory 1617, Cole Blvd, Golden, CO 80401
- [18] Hansen M O L 2008 *Aerodynamics of wind turbines* 2nd ed (London: Earthscan)
- [19] Kassapoglou C 2010 *Buckling of Composite Plates* (John Wiley & Sons, Ltd) pp 119–144 ISBN 9780470972700 URL <http://dx.doi.org/10.1002/9780470972700.ch6>
- [20] Resor B R 2013 Definition of a 5MW / 61 . 5m wind turbine blade reference model. Tech. Rep. April
- [21] Hansen M, Hansen A, Larsen T, Øye S, Sørensen P and Fuglsang P 2005 *Control design for a pitch-regulated, variable speed wind turbine* ISBN 87-550-3409-8
- [22] 2005 *International Standard IEC 61400-1* (IEC)
- [23] The MathWorks Inc. Natick, MA *MATLAB 2015b*
- [24] Han Z, Zhang K, Song W and Liu J 2013 *Aerospace Sciences Meetings* (American Institute of Aeronautics and Astronautics)
- [25] Sessarego M, Ramos-García N, Yang H and Shen W Z 2016 *Renewable Energy* **93** 620 – 635 ISSN 0960-1481 URL <http://www.sciencedirect.com/science/article/pii/S0960148116302117>
- [26] Forrester A I J, Sóbester A and Keane A J 2008 *Engineering Design via Surrogate Modelling: A Practical Guide* (John Wiley & Sons, Ltd) ISBN 9780470770801 URL <http://dx.doi.org/10.1002/9780470770801>